FEBS Letters 580 (2006) 4905–4910

Interactions of daidzin with intramolecular G-quadruplex

Wei Li[a], Ming Zhang[a], Jin-li Zhang[b,*], Hui-qing Li[c], Xiao-chen Zhang[a], Qian Sun[a], Chun-mei Qiu[b]

[a] *Department of Chemical Technology, School of Chemical Engineering and Technology, Tianjin University, Tianjin 300072, China*
[b] *Department of Biochemical Engineering, School of Chemical Engineering and Technology, Tianjin University, Tianjin 300072, China*
[c] *Shandong Academy of Medical Sciences, Jinan 250062, Shangdong Province, China*

Received 9 January 2006; revised 6 July 2006; accepted 1 August 2006

Available online 14 August 2006

Edited by Veli-Pekka Lehto

Abstract The potential interaction of daidzin, an ingredient of soy isoflavones, with human telomeric antiparallel G-quadruplex $dAG_3(T_2AG_3)_3$ was studied using ESI-MS, PAGE, CD and molecular simulation. Experimental studies indicated that daidzin molecules interacted with $dAG_3(T_2AG_3)_3$ and formed DNA–daidzin complex with the stoichiometric ratio of 1:1 and 1:2. The transition temperature of the G-quadruplex increased at higher ratio of daidzin to DNA. Under molecular crowding conditions the interactions between daidzin and the G-quadruplex become much stronger. Combining computational simulation and experimental results, it is demonstrated that the $dAG_3(T_2AG_3)_3$/daidzin complex with a stoichiometric ratio of 1:1 is stabilized through the π–π conjugacy interactions and hydrogen bondings between daidzin and the bases of G-quadruplex. This work provides guidance not only on exploring the molecular anti-cancer mechanism of dietary isoflavones, but also searching small natural products as promising anticancer candidates that can inhibit telomerase activity.

Keywords: Daidzin; Isoflavones; G-quadruplex; Molecular-crowding conditions; Anticancer

1. Introduction

Natural compounds have been intensively studied as new anticancer drugs. Genistein and daidzein, together with their respective glycoside conjugates of genistin and daidzin, are the main components of dietary soy isoflavones. They have been reported to inhibit the tumor cell growth in vivo and in vitro for breast cancer and prostate cancers [1–4]. We have recently shown that soybean isoflavone can induce the apoptosis of esophageal cancer cells EC-9706 [5]. The biological properties of genistein and genistin have been extensively investigated because of its activity as a tyrosine kinase inhibitor, possible anti-oxidant and potential anti-cancer compound [6,7]. However, the main cellular target of isoflavone constituents is yet elusive.

G-quadruplex DNA has been linked to mechanisms that relate to a number of diseases via interfering with telomere maintenance by telomerase [8–10]. Small molecules able to induce and/or stabilize G-quadruplex structures have been intensively studied for their ability to inhibit telomerase activity and act as potential anticancer agents. A number of such promising molecules have been characterized, ranging from the derivatives of anthraquinones [11], porphyrins [12], acridines[13], perylenes [14] and triazines [15,16], to natural compounds such as telomestatin [17], ascididemin [18], and alkaloid berberine [19]. External stacking, intercalation and non-specific binding are possible modes for such planar aromatic molecules binding to the antiparallel quadruplex [20–22].

The recent discovery of the above-mentioned natural compounds that interact with G-quartet, especially ascididemin that is a conventional Topo II poison and berberine that is an antibiotic from herb medicine, motivated us to test the potential interaction of isoflavones with G-quadruplex. This article investigated potential interactions of daidzin with the human/vertebrate telomeric repeat oligonucleotides $dAG_3(T_2AG_3)_3$ and $d(C_3TA_2)_3C_3T$ using molecular docking simulation and characterization through ESI-MS, PAGE and CD. Combining with the control experiment involving curcumin under molecular crowding conditions, the experimental results reflect that daidzin can interact with the antiparallel G-quadruplex AG-22 and form AG-22/daidzin complex with the stoichiometric ratio of 1:1 and 1:2. The molecular simulation suggests that daidzin is preferably bound in the diagonal loop region of the G-quadruplex. This is the first report on the interactions of daidzin with G-rich telomeric DNA, suggesting that it may serve as another molecular action pathway for dietary isoflavones to exert their anticancer effects.

2. Materials and methods

Oligonucleotides $dAG_3(T_2AG_3)_3$ (AG-22, 6966 Da) and $d(C_3TA_2)_3C_3T$ (CT-22, 6504 Da) were purchased from the Japanese Takara Bio (Dalian) with the purity higher than 98% measured by the reversed-phase high performance liquid chromatography (HPLC). Daidzin and curcumin were purchased from Sigma and were used without further purification.

2.1. Mass spectrometry

Electrospray ionization mass spectrometry (ESI-MS) was utilized to investigate the binding stoichiometry of small molecule to the G-quadruplex and the duplex. Mass spectra were obtained on a Thermo Finnigan LCQ Advantage in the negative ion mode. Ammonium acetate was chosen as the electrolyte for its compatibility with electrospray mass spectrometry. DNA solutions were prepared in 150 mM NH_4OAC buffer (pH 7.0) with and without 50 μM daidzin, respectively, and were heated to 95 °C for 10 min then cooled overnight to 4 °C. The DNA conformation in ammonium acetate was

*Corresponding author. Fax: +86 22 27890014.
E-mail address: zhangjinli@tju.edu.cn (J. Zhang).

0014-5793/$32.00
doi:10.1016/j.febslet.2006.08.007

proved to be the same as in 100 mM Na^+ buffers (pH 7.0) by using circular dichroism experiments. The experimental conditions were optimized to avoid denaturation of the duplex and the quadruplex species: the heated capillary temperature of the electrospray source was set to 185 °C, and a voltage on the heated capillary of −11 V. Full scan MS spectra were recorded in a *m/z* range from 800 to 2000, and 50 scans were summed for each spectrum. The relative intensities of the free and bound DNA in the mass spectra are assumed to be proportional to the relative abundances of these species in solution [23].

2.2. Circular dichroism

CD experiments were carried out to analyze the conformation and stability of DNA sequences. CD spectra were obtained with a Jacso J-810 spectropolarimeter equipped with a Julabo temperature controller. All the CD spectra were measured at total strand concentration of 50 μM DNA in a 0.1-cm path length cuvette with 90 mM Tris–borate buffer containing 100 mM Na^+ (pH 7.0). Each sample was scanned at least three times to get the average data curves from the wavelength of 200 to 350 nm. The scan of the buffer alone was subtracted from the average scan for each sample. The cell holding chamber was flushed with a constant stream of dry nitrogen gas to avoid water condensation on the cell exterior.

Melting curves of the G-quadruplex AG-22 and the duplex AG-22/CT-22 were measured at 295 and 265 nm, respectively. Thermal denaturation profiles were collected in units of millidegrees as a function of temperature. The heating rate was fixed at 1.0 °C/min. All samples were annealed by heating the sample cuvette to 95 °C for 10 min and then cooling to 4 °C.

2.3. Polyacrylamide gel electrophoresis (PAGE)

The gel electrophoresis mobility shift assay was used to characterize the DNA–daidzin interactions in 90 mM Tris–borate buffer (pH 7.0) at the presence of 100 mM Na^+. The same buffer was used in the polymerization of the acrylamide for the relevant gels. DNA samples with a total strand concentration of 10 μM were annealed by heating to 90 °C for 5 min, cooling to 4 °C, and incubating at this temperature for several hours. Electrophoresis was carried out using 20% acrylamide [29:1 acrylamide/bis(acrylamide)] at 8 V/cm and 4 °C for 8 h. The gel was stained in a 1 μg/mL ethidium bromide solution for 30 min.

2.4. Molecular modeling

Sybyl modeling software version 6.9 (Tripos Inc., St. Louis, MO) using Gasteiger–Marsili charges, Tripos force field and conjugate gradients was employed for the calculation. Coordinates for the AG-22 quadruplex were obtained from the Brookhaven Protein Data Bank (PDB entry 143D). Molecular mechanics energy minimization (2000 steps) followed by dynamics (1 fs step, 50 ps at 298 K) and subsequent mechanics (minimization of time-averaged dynamics structure) was used. Daidzin molecule was respectively docked in the diagonal loop or the groove of the G-quadruplex, or intercalated between the G-tetrads using DOCKING module of the Sybyl 6.9 package. The complex molecule was surrounded by a periodic box of water molecules described by the TIP3P potential extended to a distance of 10 Å from any solute atom, followed by equilibration with the solvent molecules (2000 steps of minimization and 20 ps of restrained molecular dynamic at 298 K). The resulting complex was then subjected to a series of minimization and dynamics calculation in which the constraints were gradually relaxed. The final production run was performed without any constraints on the complex for 500 ps and coordinates were saved after every 50 fs for analysis of their trajectories.

Relative binding energy was calculated according to Eq. (1), where $E_{complex}$ denotes the total energy of the DNA–daidzin complex,

$$E_{bind} = E_{complex} - E_{receptor} - E_{ligand}, \quad (1)$$

$E_{receptor}$ and E_{ligand} is the energy of the single G-quadruplex DNA and the small molecular daidzin, respectively. Although these calculated energies are not identical to absolute thermodynamic binding energies measured by biophysical methods, it is indicated that this approach provides estimated relative binding interaction energies for ligand substitutions, which do correlate with biochemical measurements data [24].

3. Results and discussion

3.1. Detection of daidzin–quadruplex complex

ESI-MS is a highly sensitive method to study the interactions of drugs with DNA duplex, triplex and quadruplex structures [25–27]. In the present work, the negative mode electrospray mass spectrometry confirmed that daidzin can

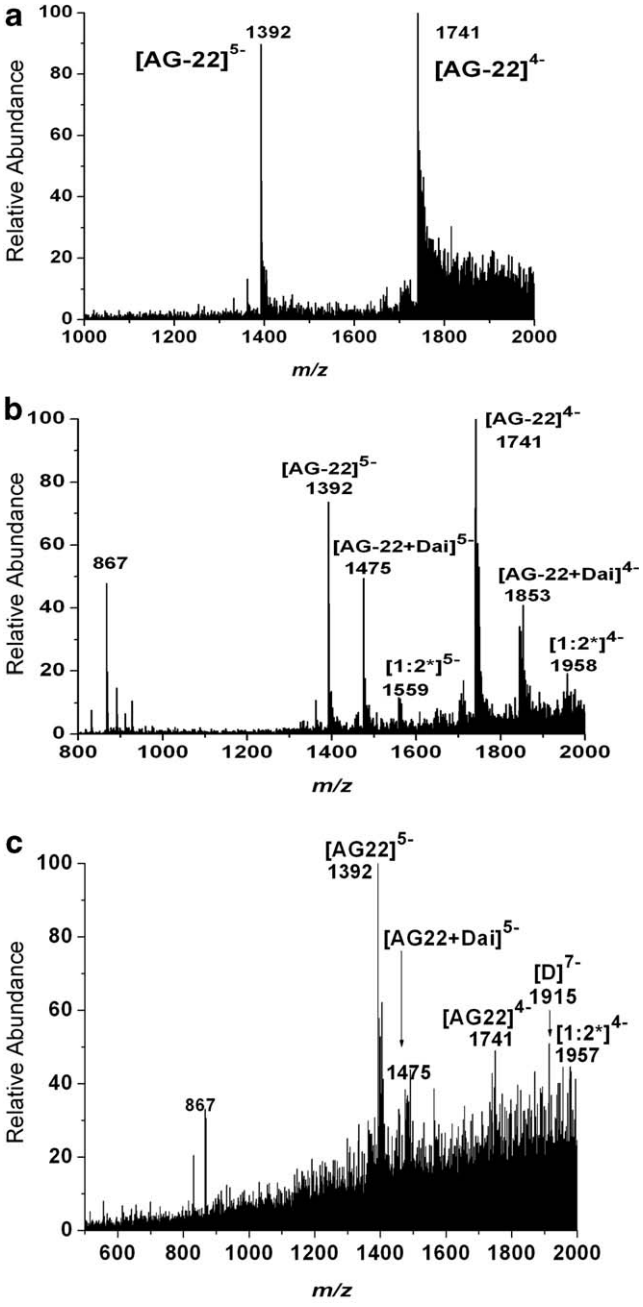

Fig. 1. ESI-MS spectra of 5 μM AG-22 alone (a), the mixture of 50 μM daidzin and 5 μM AG-22 (b), and the mixture of 50 μM daidzin and 5 μM double-stranded AG-22/CT-22 (c) in 150 mM NH_4OAC buffers (pH 7.0). The *m/z* ratios were marked for relative high abundance species in the spectra. $[AG\text{-}22]^{5-}$ and $[AG\text{-}22]^{4-}$ referred to the species of G-quadruplex AG-22 with the charge of negative five and four, respectively. [AG-22+Dai] referred to the species of the AG-22/daidzin complex with a ratio of 1:1, and [1:2*] to the species with the AG-22/daidzin ratio of 1:2. $[D]^{7-}$ referred to the species of duplex AG-22/CT-22 with the charge of negative seven.

form complexes with the G-quadruplex. Fig. 1 illustrates typical ESI-MS spectra of AG-22, AG-22/daidzin mixture, and equimolar mixture of AG-22 and CT-22 (AG-22/CT-22) together with daidzin in 150 mM NH_4OAC buffer (pH 7.0).

Analysis of the MS spectra based on the molecular weight of AG-22 indicates that the charge of the species at the *m*/*z* ratio of 1392 is negative five and that at the *m*/*z* ratio of 1741 is negative four (as shown in Fig. 1a). In the MS spectra of AG-22/daidzin mixtures (Fig. 1b), the most abundant species are located at the *m*/*z* ratio of 1475 with a charge of negative five and at 1853 with a charge of negative four, besides two species of AG-22 at the ratio of 1392 and 1741 as mentioned above. The difference of the molecular weight between the species at the ratio of 1392 and that at 1475 is 416, just equal to the molecular weight of daidzin. Comparing another two species located at the ratio of 1853 and at 1741 with the charge of negative four, the difference of their molecular weight equals 448, which is approximately equal to the summation of molecular weight of one daidzin and two ammonium ions. Similarly, Rosu et al. also concluded that the shift of molecular weight was due to the existence of ammonium ions located between the G-tetrad planes through characterization of the mixture of ethidium derivatives and G-quadruplex by using ESI-MS [23]. Additionally in the MS spectra of AG-22/daidzin mixtures, the two species located at the *m*/*z* ratio of 1559 and 1958 illuminate that there exists the AG-22/daidzin complex with a stoichiometric ratio of 1:2.

It deserves to be mentioned that the AG-22/daidzin complex with the stoichiometric ratio of both 1:1 and 1:2 can be still detected in the mixture of double-stranded AG-22/CT-22 and daidzin (as shown in Fig. 1c). For the double-stranded AG-22/CT-22 alone, the MS spectra reflected the existence of the single-stranded AG-22 and CT-22, as well as the double-stranded duplex (Figure S1 in the Supporting Materials). However, there was no detection of the species corresponding to the complex of the duplex and daidzin (Fig. 1c).

The electrophoretic mobility shift assay for the double-stranded AG-22/CT-22 and single-stranded AG-22 gave results in accord with the ESI-MS. Figs. 2a and b show, respectively, the native PAGE images for the duplex and the single-stranded AG-22 in the presence of various concentration of daidzin under the same buffer condition. As the ratio of daidzin to DNA ranged from 0 to 10, the electrophoretic mobility of the double-stranded mixture was independent of the daidzin concentration in each lane where a band was assigned to the Watson-Crick duplex of AG-22/CT-22, whereas AG-22 showed an obviously slower mobility at higher daidzin concentrations. The slower mobility of AG-22 should be attributed to the complex structure of AG-22 and the ligand of daidzin.

3.2. Effect of daidzin on G-quadruplex stability

The conformational characteristics of the G-quadruplex were detected by CD spectra in the absence and in the presence of daidzin, respectively. CD spectra of the sequence AG-22 showed a positive peak at 295 nm and the negative peak at 263 (as shown in Fig. 3a), which is the characteristic of anti-paralleled G-quadruplexes [28]. As the daidzin concentration increased, the height of both peaks increased along with a blue-shift of the peak at 295 nm.

Thermal denaturation profiles were further used to study the effect of daidzin on the G-quadruplex stability. As the ratio of

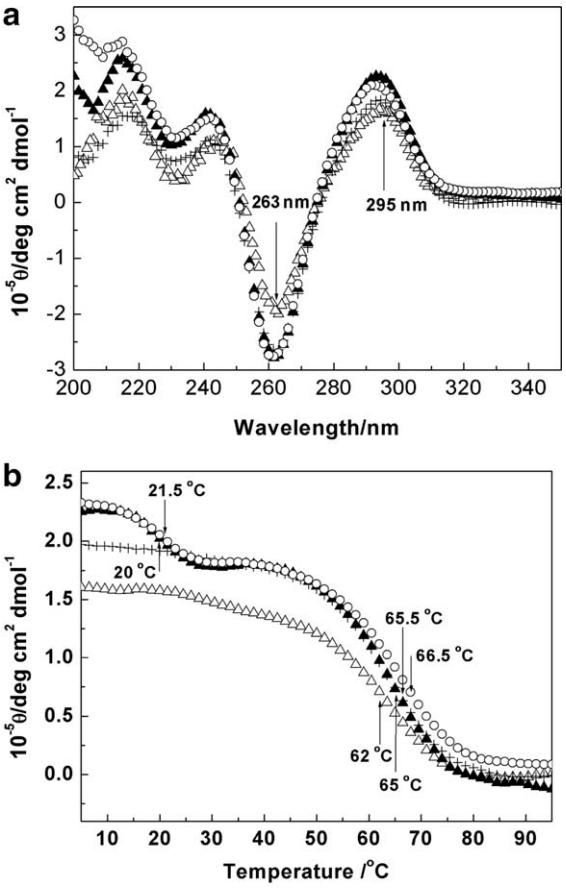

Fig. 3. (a) CD spectra of 50 μM AG-22 in 100 mM Na^+ buffers (△), and with different concentration of daidzin: 10 μM daidzin (+), 25 μM daidzin (▲), 100 μM daidzin (○), respectively. (b) CD melting profiles of 50 μM AG-22 in 100 mM Na^+ buffers (△), and with different concentration of daidzin: 10 μM daidzin (+), 25 μM daidzin (▲), 100 μM daidzin (○), respectively.

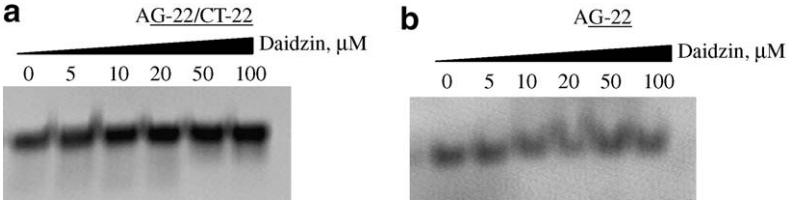

Fig. 2. PAGE images of the double-stranded AG-22/CT-22 (a) and the single-stranded AG-22 alone (b) with different concentration of daidzin. Daidzin was titrated against 10 μM DNA in 90 mM TB buffer (100 mM Na^+ and pH 7.0). The major band was identified as the duplex in the double-strand mixture (a), and as the G-quadruplex in the single-strand AG-22 system (b).

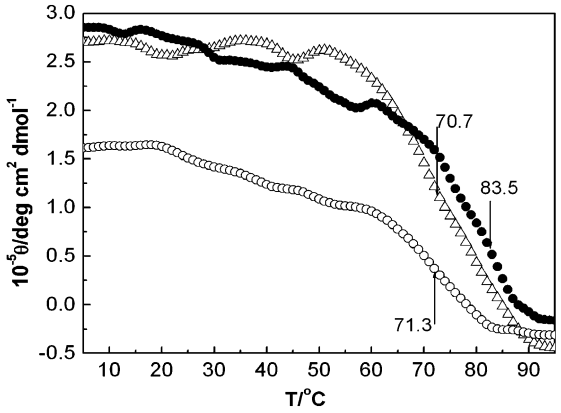

Fig. 4. CD Melting profiles of 50 μM AG-22 under the molecular-crowding condition of 400 g/L PEG solutions in the presence of 100 mM Na^+ buffers (△), 50 μM Daidzin solutions (●), or 50 μM curcumin solutions (○), respectively.

daidzin to AG-22 equaled 2, the transition temperature of the G-quadruplex increased from 62.0 to 66.5 °C (as shown in Fig. 3b). Moreover, when the concentration of daidzin was higher than 25 μM, there appeared a second structural transition around the temperature of 21 °C. This second conformational transition further confirmed the existence of the AG-22/daidzin complex with different stoichiometric ratios as indicated through the ESI-MS. However, this second complex is not so stable as the AG-22/daidzin with a stoichiometric ratio of 1:1. In the case of the duplex of AG-22/CT-22, CD spectra in the presence of daidzin were similar to those in 100 mM Na^+ buffers (Figure S2 in Supporting Information). And the melting curves indicated that daidzin had no effects on the transition temperature of the duplex AG-22/CT-22 (Figure S3 in Supporting Information), which suggest no substantial interactions of daidzin with the duplex.

As a control, we also studied the effect of curcumin, another natural compound with aromatic rings structure, on the G-quadruplex. Curcumin (as shown by Figure S4 in Supporting Information) is an active ingredient from the spice turmeric (Curcuma longa Linn), which is reported to have inhibitory effects on telomerase activity in human mammary epithelial and breast cancer cells [29]. Both CD spectra and melting profiles (Figure S5 in Supporting Information) indicated that curcumin had no effect on the conformation and the stability of the G-quadruplex AG-22.

The condition in a living cell is inherently molecule-crowded with biomacromolecules such as nucleic acids, proteins, and polysaccharides. It has been reported that molecular crowding dramatically stimulates the association between biomolecules and induces the structural polymorphism of the telomeric DNAs [30–32]. The inert 4 kDa polyethylene glycol (PEG)

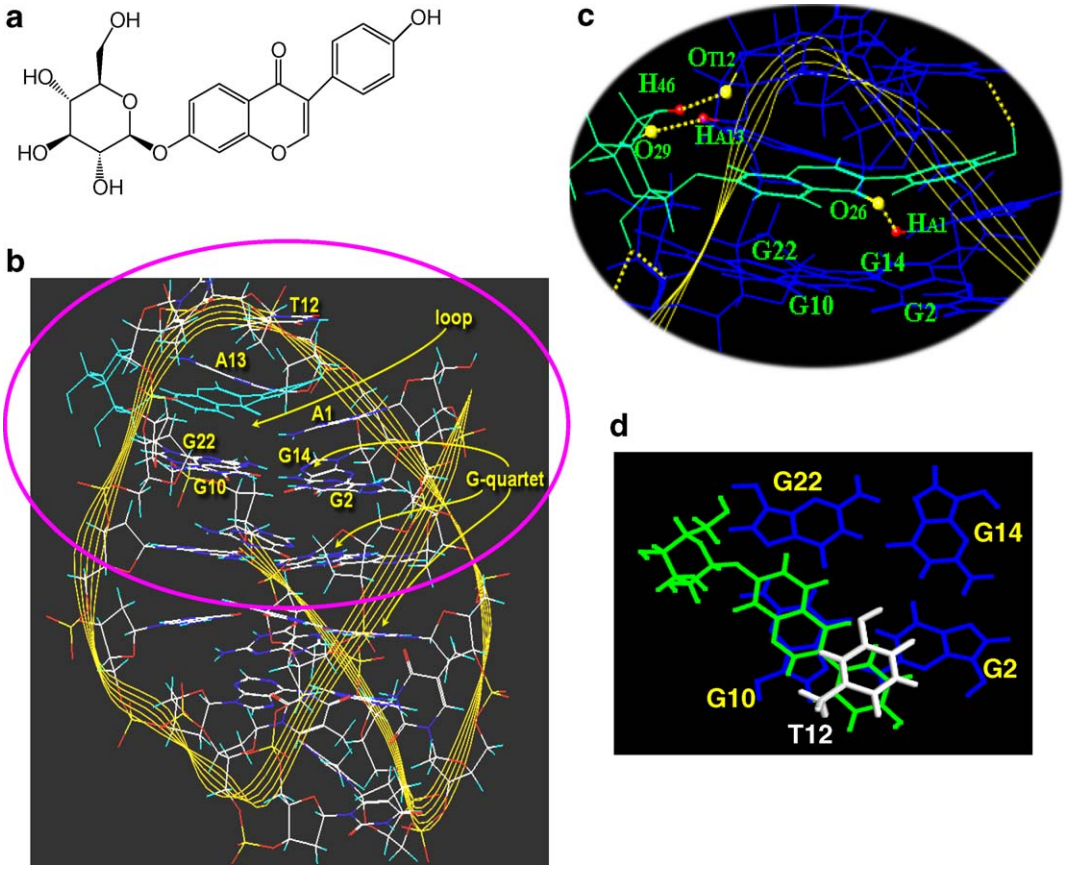

Fig. 5. (a) Molecular formula of daidzin. (b) The stable docking model of daidzin bound in a stacking mode to the loop of the human telomeric G-quadruplex AG-22. (c) A magnified image of the upper side of (b). It shows six hydrogen bonding interactions of daidzin with the G-quadruplex, among which three strong hydrogen bondings are O3–T12···O25–Daidzin, O29–Daidzin···N17–A13, and O26–Daidzin···N14–A1, respectively. The small red points indicate donors of hydrogen bondings and the large yellow points are acceptors. (d) The top view of the molecule of daidzin forming π–π conjugacy interactions with the base G10 and T12 of AG-22.

was added into the same medium in order to mimic the molecular crowding condition. Under the crowding condition the transition temperature of AG-22/Daidzin complex is up to 83.5 °C at the ratio of 1:1 (as shown in Fig. 4), which is about 13 °C higher than that of the AG-22 under the same condition. Fig. 4 also shows the melting curve of the curcumin/AG-22 mixtures under crowding conditions, which displays almost the same transition temperature as AG-22. This result shows that much stronger interactions exist between the natural molecule daidzin and the telomeric G-quadruplex of AG-22 with the aid of macromolecular crowding environment.

3.3. Molecular modeling of the daidzin–quadruplex complex

A docking simulation was adopted to study the interactions between daidzin and the G-quadruplex of AG-22. The initial DNA model is adopted from the PDB entry 143D, which is the conformation of G-quadruplex in the presence of sodium ion. Three possible modes were simulated for the complex of AG-22/daidzin with a ratio of 1:1, i.e., daidzin externally stacked in the diagonal loop region, intercalated between the G-tetrad planes, or bound in the groove of the G-quadruplex. The negative value of the binding energy suggests favorable formation of a stable complex of AG-22/daidzin in which one daidzin molecule binds in the diagonal loop region of G-quadruplex through the external stacking with the G-tetrad. The minimized energy of the daidzin/DNA complex ($E_{complex}$), the single receptor of DNA ($E_{receptor}$) and the ligand of daidzin (E_{ligand}) equalled to −146.330, −111.891, 31.983 kcal/mol, respectively. Then the binding energy of daidzin and the G-quadruplex AG-22 was calculated to be −66.442 kcal/mol.

Fig. 5 shows a stable model for the daidzin–DNA complex in which daidzin is located in the diagonal loop of G-qudruplex AG-22 (Fig. 5b). In the final minimized structure, the middle aromatic rings of daidzin molecule form π–π conjugacy interactions with the bases of G10 and T12 of AG-22 (as shown in Fig. 5d), and the terminal atoms of daidzin form hydrogen bondings with the base atoms of G-quadruplex. Fig. 5c indicates three hydrogen bondings each has a bonding distance between 2.4 and 3.0 Å, i.e., O3–T12···O25–Daidzin, O29–Daidzin···N17–A13, and O26–Daidzin···N14–A1, where the former part indicates the oxygen acceptor group of the hydrogen bonds, and the latter is the donor group. For instance, O3–T12···O25–Daidzin means that the oxygen atom No. 3 (O3) in the thymine base No.12 (T12) of the AG-22 forms hydrogen bonding with the hydrogen atom (H46) connected with the oxygen atom No. 25 (O25) of Daidzin.

Combining computational simulation and experimental studies, it is demonstrated that the $dAG_3(T_2AG_3)_3$/daidzin complex with a stoichiometric ratio of 1:1 is stabilized through the π–π conjugacy interactions and hydrogen bondings between daidzin and the bases of G-quadruplex. This first report on the interactions of daidzin with G-rich telomeric DNA can promote not only studies on the molecular anti-cancer mechanism of dietary isoflavones, but also searching small natural products as promising anticancer candidates that can inhibit telomerase activity.

4. Conclusion

The present work explored the interactions of daidzin, one of components of soy isoflavones, with telomeric oligonucleotide $dAG_3(T_2AG_3)_3$ in the presence of 100 mM Na^+ buffer at molecular level using ESI-MS, PAGE, CD and molecular simulation. Experimental studies indicated that the existence of the $dAG_3(T_2AG_3)_3$/daidzin complex with the stoichiometric ratio of 1:1 and 1:2, and the transition temperature of the G-quadruplex increased at higher ratio of daidzin to DNA. As a control another natural compound, curcumin, was studied. These results indicated that the interactions between daidzin and the antiparallel G-quadruplex $dAG_3(T_2AG_3)_3$ become much stronger under molecular crowding conditions. The molecular simulation for the $dAG_3(T_2AG_3)_3$/daidzin complex with a stoichiometric ratio of 1:1 revealed that there exist π–π conjugacy interactions and hydrogen bondings between daidzin and the bases of G-quadruplex. This work on interactions of daidzin with the telomeric G-quadruplex can provide guidance not only on studying the molecular anti-cancer mechanism of dietary isoflavones, but also searching natural products as promising anticancer candidates that can inhibit telomerase activity.

Acknowledgments: We greatly appreciate Dr. Yi Lu, Professor of Chemistry and Biochemistry in University of Illinois, Urbana-Champaign, for his kind modification for this article. The work described here is sponsored by the SRF for ROCS, the NSFC (Nos. 20476077 and 20576090), the PCSIRT and the ChunHui Project.

Appendix A. Supplementary data

Supplementary data associated with this article can be found, in the online version, at doi:10.1016/j.febslet.2006.08.007.

References

[1] Barnes, S., Grubbs, C., Setchell, K.D. and Carlson, J. (1990) Soybeans inhibit mammary tumors in models of breast cancer. Prog. Clin. Biol. Res. 347, 239–253.
[2] Kyle, E., Neckers, L., Takimoto, C., Curt, G. and Bergan, R. (1997) Genistein-induced apoptosis of prostate cancer cells is preceded by a specific decrease in focal adhesion kinase activity. Mol. Pharmacol. 51, 193–200.
[3] Polkowski, K. and Mazurek, A.P. (2000) Biological properties of genistein. A review of in vitro and in vivo data. Acta Pol. Pharm. 57, 135–155.
[4] Popiolkiewicz, J., Polkowski, K., Skierski, J.S. and Mazurek, A.P. (2005) In vitro toxicity evaluation in the development of new anticancer drugs – genistein glycosides. Cancer Lett. 229, 67–75.
[5] Ma, J.X., Su, J.Y., Ma, J.S., Li, H.Q. and Yan, Y. (2003) Study on the molecular mechanism of apoptosis in esophageal cancer cells induced by soybean isoflavone. Chin. J. Epidemiol. 24, 1040–1043.
[6] Ravindranath, M.H., Muthugounder, S., Presser, N. and Viswanathan, S. (2004) Anticancer therapeutic potential of soy isoflavone, genistein. Adv. Exp. Med. Biol. 546, 121–165.
[7] Magee, P.J. and Rowland, I.R. (2004) Phyto-oestrogens, their mechanisms of action: current evidence for a role in breast and prostate cancer. Br. J. Nutr. 91 (4), 513–531.
[8] Neidle, S. and Parkinson, G. (2002) Telomere maintenance as a target for anticancer drug discovery. Nat. Rev. Drug Discovery 1, 383–393.
[9] Siddiqui-Jian, A., Grand, C.L., Bearss, D.J. and Hurley, L.H. (2002) Direct evidence for a G-quadruplex in a promoter region and its targeting with a small molecule to repress c-MYC transcription. Proc. Natl. Acad. Sci. USA 99, 11593–11598.
[10] Zaug, A.J., Podell, E.R. and Cech, T.R. (2005) Human POT1 disrupts telomeric G-quadruplexes allowing telomerase extension *in vitro*. Proc. Natl. Acad. Sci. USA 102, 10864–10869.

[11] Sun, D., Thompson, B., Cathers, B.E., Salazar, M., Kerwin, S.M., Trent, J.O., Jenkins, T.C., Neidle, S. and Hurley, L.H. (1997) Inhibition of human telomerase by a G-quadruplex-interactive compound. J. Med. Chem. 40, 2113–2116.
[12] Seenisamy, J., Bashyam, S., Gokhale, V., Vankayalapati, H., Sun, D., Siddiqui-Jain, A., Streiner, N., Shin-Ya, K., White, E., Wilson, W.D. and Hurley, L.H. (2005) Design and synthesis of an expanded porphyrin that has selectivity for the c-MYC G-quadruplex structure. J. Am. Chem. Soc. 127, 2944–2959.
[13] Burger, A.M., Dai, F., Schultes, C.M., Reszka, A.P., Moore, M.J., Double, J.A. and Neidle, S. (2005) The G-quadruplex-interactive molecule BRACO-19 inhibits tumor growth, consistent with telomere targeting and interference with telomerase function. Cancer Res. 65, 1489–1496.
[14] Fedoroff, O.Y., Salazar, M., Han, H., Chemeris, V.V., Kerwin, S.M. and Hurley, L.H. (1998) NMR-based model of a telomerase-inhibiting compound bound to G-quadruplex DNA. Biochemistry 37, 12367–12374.
[15] Riou, J.F., Guittat, L., Mailliet, P., Laoui, A., Renou, E., Petitgenet, O., Megnin-Chanet, F., Helene, C. and Mergny, J.L. (2002) Cell senescence and telomere shortening induced by a new series of specific G-quadruplex DNA ligands. Proc. Natl. Acad. Sci. USA 99, 2672–2677.
[16] Fletcher, T.M. (2005) Telomerase: a potential therapeutic target for cancer. Expert. Opin. Ther. Targets 9, 457–469.
[17] Kim, M., Vankayalapati, H., Shin-ya, K., Wierzba, K. and Hurley, L.H. (2002) Telomestatin, a potent telomerase inhibitor that interacts quite specifically with the human telomeric intramolecular G-quadruplex. J. Am. Chem. Soc. 124, 2098–2099.
[18] Guittat, L., De Cian, A., Rosu, F., Gabelica, V., De Pauw, E., Delfourne, E. and Mergny, J.L. (2005) Ascididemin and meridine stabilise G-quadruplexes and inhibit telomerase in vitro. Biochim. Biophys. Acta 1724, 375–384.
[19] Franceschin, M., Rossetti, L., D'Ambrosio, A., Schirripa, S., Bianco, A., Ortaggi, G., Savino, M., Schultes, C. and Neidle, S. (2006) Natural and synthetic G-quadruplex interactive berberine derivatives. Bioorg. Med. Chem. Lett. 16, 1707–1711.
[20] Mergny, J.L., Lacroix, L., Teulade-Fichou, M.P., Hounsou, C., Guittat, L., Hoarau, M., Arimondo, P.B., Vigneron, J.P., Lehn, J.M., Riou, J.F., Garestier, T. and Helene, C. (2001) inhibitors based on quadruplex ligands selected by a fluorescence assay. Proc. Natl. Acad. Sci. USA 98, 3062–3067.
[21] Shi, D.F., Wheelhouse, R.T., Sun, D. and Hurley, L.H. (2001) Quadruplex-interactive agents as telomerase inhibitors: synthesis of porphyrins and structure–activity relationship for the inhibition of telomerase. J. Med. Chem. 44, 4509–4523.
[22] Read, M., Harrison, R.J., Romabnoli, B., Tanious, F.A., Gowan, S.H., Reszka, A.P., Wilson, W.D., Kelland, L.R. and Neidle, S. (2001) Structure-based design of selective and potent G quadruplex-mediated telomerase inhibitors. Proc. Natl. Acad. Sci. USA 98, 4844–4849.
[23] Rosu, F., De Pauw, E., Guittar, L., Alberti, P., Lacroix, L., Mailliet, P., Riou, J.F. and Mergny, J.L. (2003) Selective interaction of ethidium derivatives with quadruplexes: an equilibrium dialysis and electrospray ionization mass spectrometry analysis. Biochemistry 42, 10361–10371.
[24] Read, M.A., Wood, A.A., Harrison, J.R., Gowan, S.M., Kelland, L.R., Dosanjh, H.S. and Neidle, S. (1999) Molecular modeling studies on G-quadruplex complexes of telomerase inhibitors: structure–activity relationships. J. Med. Chem. 42, 4538–4546.
[25] Gabelica, V., De Pauw, E. and Rosu, F. (1999) Interaction between antitumor drugs and a double-stranded oligonucleotide studied by electrospray ionization mass spectrometry. J. Mass Spectromet. 34, 1328–1337.
[26] Rosu, F., Gabelica, V., Houssier, C., Colson, P. and De Pauw, E. (2002) Triplex and quadruplex DNA structures studied by electrospray mass spectrometry. Rapid Commun. Mass Spectomet. 16, 1729–1736.
[27] Carraso, C., Rosu, F., Gabelica, V., Houssier, C., De Pauw, E., Garbay-Jaureguiberry, C., Roques, B., Wilson, W.D., Chaires, J.B., Waring, M.J. and Bailly, C. (2002) Tight binding of the antitumor drug ditercalinium to quadruplex DNA. ChemBioChem 3, 1235–1241.
[28] Li, W., Miyoshi, D., Nakano, S. and Sugimoto, N. (2003) Structural competition involving G-quadruplex DNA and its complement. Biochemistry 42, 11736–11744.
[29] Ramachandran, C., Fonseca, H.B., Jhabvala, P., Escalon, E.A. and Melnick, S.J. (2002) Curcumin inhibits telomerase activity through human telomerase reverse transcritpase in MCF-7 breast cancer cell line. Cancer Lett. 184, 1–6.
[30] Minton, A.P. (2001) The influence of macromolecular crowding and macromolecular confinement on biochemical reactions in physiological media. J. Biol. Chem. 276, 10577–10580.
[31] Ellis, R.J. (2001) Macromolecular crowding: an important but neglected aspect of the intracellular environment. Curr. Opin. Struct. Biol. 11, 114–119.
[32] Miyoshi, D., Matsumura, S., Nakano, S. and Sugimoto, N. (2004) Duplex dissociation of telomere DNAs induced by molecular crowding. J. Am. Chem. Soc. 126, 165–169.